

Self-phase-modulation in silica optical fibers

R. H. Stolen and Chinlon Lin

Bell Telephone Laboratories, Holmdel, New Jersey 07733

(Received 10 October 1977)

We report measurements of frequency broadening due to self-phase-modulation (SPM) in optical fibers. The use of single-mode silica-core fibers and mode-locked argon-laser pulses leads to the simplest and cleanest measurements yet made of SPM. The qualitative features of the frequency spectrum are in good agreement with theoretical expectations. The experiment provides an independent measurement of n_2 , the self-focusing coefficient. The results also point to some simple and useful techniques based on fibers for the measurement and analysis of mode-locked laser pulses.

I. INTRODUCTION

An intensity-dependent refractive index leads to self-focusing and phase modulation within a single optical pulse. In fibers, any additional confinement caused by self-focusing is negligible, but a small phase retardation at the peak of the pulse with respect to the leading and trailing edges will add up in a long fiber and result in sizable phase modulation. The frequency broadening associated with this phase modulation will, in combination with group-velocity dispersion, increase the pulse spreading. Since pulse spreading limits the information rate in a fiber transmission system, self-phase-modulation will be an important power-limiting nonlinear process in high-capacity single-mode fibers.

Self-phase-modulation (SPM) was first observed as a modulated spectrum extending both above and below the laser frequency after self-focusing had occurred in a liquid-filled cell and was explained as phase modulation due to the intensity dependent refractive index by Shimizu.¹ Because this process took place in self-focused filaments, the intensity was high and there were problems with competing nonlinear effects and uncertainties concerning the filament size. Self-phase-modulation was obtained in the absence of self-trapping or self-focusing and at low powers by using CS₂-filled glass fibers.² Analysis of the measured frequency spectrum was complicated, however, because of the multimode nature of the liquid-filled fiber and because the 2.5-ps half-width of the optical pulse was comparable to the relaxation time of the nonlinearity in CS₂.

In this paper we report measurements of frequency broadening of mode-locked argon-laser pulses due to SPM in single-mode silica-core fibers. Because of the stability of the system it was possible to slowly increase the optical power and observe clearly the development of the broadened spectrum. Analysis is simplified because the re-

laxation time of the nonlinearity in glass is much faster than the pulse length.³ The qualitative features of the frequency spectrum are in good agreement with theoretical expectations and the measured nonlinear coefficient agrees well with values obtained by other techniques. Typically, in our 100-m single-mode fibers the frequency bandwidth increases by a factor of 10 for a peak power of about 3 W.

II. EXPERIMENTAL

The experimental arrangement is illustrated in Fig. 1. The argon-ion laser operates at 514.5 nm and is mode-locked with an acousto-optic cell and rf driver. Reflections from the lenses and fiber ends as well as backward scattered Rayleigh light from the fiber broaden the mode-locked pulse so an isolator consisting of a Faraday rotator and two polarizers was inserted between the laser and fiber. Light is coupled in and out of the fiber with 20× microscope objectives.

Measurements were made on two silica-core, borosilicate-clad fibers. The first fiber was 116 m long and had a core diameter of 4.5 μm, a characteristic number V^4 of 4.0, and a loss at 514.5 nm of 32 dB/km. While this fiber supported two modes it was possible by careful coupling to excite only the fundamental LP_{01} mode. The second fiber was 99 m long with a 3.35-μm core diameter, a V number of 2.53, and a loss of 17 dB/km.

The frequency spectrum of the input pulse was measured with a scanning confocal Fabry-Perot

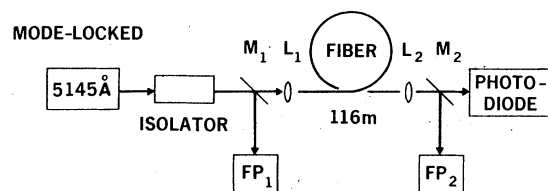


FIG. 1. Experimental arrangement.

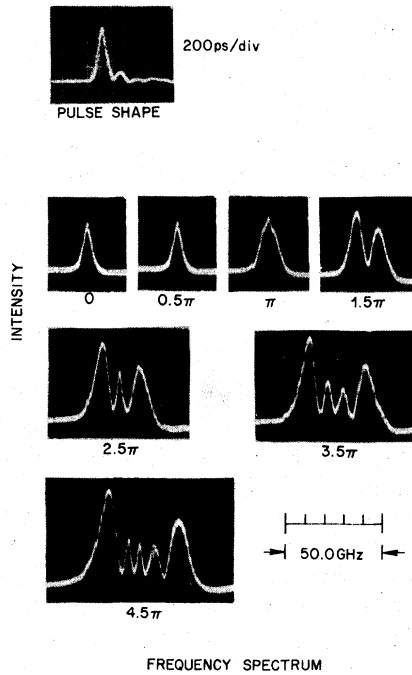


FIG. 2. Photographs of input pulse shape and the output spectrum from a 3.35- μm silica-core fiber. Spectra are labeled by the maximum phase shift which is proportional to peak power.

interferometer with a 10-GHz free spectral range. The spectrum after the fiber was measured with a piezoelectrically scanned planar Fabry-Perot which was set for a free spectral range of 115.3 GHz. The confocal Fabry-Perot resolved the individual axial modes of the mode-locked laser while the resolution of the planar Fabry-Perot was about $\frac{1}{3}$ of the laser linewidth. Figure 2 shows photographs of the output spectrum from the 3.35- μm fiber at different powers as displayed on an oscilloscope. The power was varied by changing the input coupling. Spectra are labeled by the maximum phase shift which is proportional to peak power and will be discussed in greater detail later. The unbroadened laser linewidth is 4.6 GHz (FW $1/e$).

The duration of the mode-locked pulse was measured using a silicon PIN photodiode with a response time of about 50 ps. A photograph of the pulse as seen on a sampling oscilloscope is included in Fig. 2. The measured $1/e$ pulse width is 190 ps so if we assume a Gaussian pulse and a Gaussian detector response this sets an upper limit to the pulse width of 180 ps (FW $1/e$). The lower limit is the transform of a 4.6-GHz Gaussian pulse which would be 140 ps (FW $1/e$). The pulse was measured before and after the fiber at both low and high power with no difference in pulse shape or

width observed.

The pulse length is extremely dependent on the mode-locker drive frequency. This frequency was adjusted by maximizing the width of the broadened spectrum. This was in fact a more convenient method of "peaking up" the mode locker than the conventional technique of observing the pulse duration with a fast diode and sampling oscilloscope.

After each of the photographs in Fig. 2 was taken, the average power out of the fiber was measured. The peak power at the beginning of the fiber can then be deduced from the pulse width and separation after correction for fiber loss and end reflection. Mode strippers were used at the beginning and end of the fiber to remove unwanted cladding light.

The core-cladding boundaries of the fibers were reasonably sharp and the mode profiles were approximated by the LP_{01} mode of step index fibers.⁴ The mode profile and its corresponding far field pattern were first calculated using measured values of core size and index difference. There is some uncertainty in any measurement of the core size of such small fibers and the numbers were checked by comparing measured and calculated far field patterns. This usually resulted in an increase in the value for the core diameter by about 10%.

III. FREQUENCY SPECTRUM

The frequency spectrum after self-phase-modulation is given by the Fourier transform of the pulse amplitude^{1,5,6}:

$$F(\omega) = \frac{1}{2\pi} \int_{-\infty}^{\infty} P(t)^{1/2} e^{i\Delta\phi(t)} e^{-i(\omega - \omega_0)t} dt. \quad (1)$$

The phase shift $\Delta\phi(t)$ in a lossless fiber is proportional to the fiber length L and the intensity-dependent refractive index δn which in turn is proportional to the intensity:

$$\Delta\phi(t) = (2\pi L/\lambda)\delta n, \quad (2a)$$

$$\delta n = \frac{1}{2}n_2 E^2, \quad (2b)$$

$$E^2 = 10^7 [8\pi P(t)/ncA_{\text{eff}}], \quad (2c)$$

where n_2 is the coefficient for self-focusing in esu, λ is the vacuum wavelength, n is the refractive index, E is the peak field amplitude in cgs units, and $P(t)$ is the pump power in watts.

Because of linear absorption (α) in the fiber, L is replaced by an effective length which is less than the actual fiber length:

$$L_{\text{eff}} = \int_0^L e^{-\alpha l} dl = \frac{1 - e^{-\alpha L}}{\alpha}. \quad (3)$$

The effective area A_{eff} is the same as for stimulated Raman or Brillouin scattering in a single-

mode fiber⁷ and is determined by an integral over the mode field $\psi(r, \theta)$.

$$A_{\text{eff}} = \langle \psi^2 \rangle^2 / \langle \psi^4 \rangle \quad (4)$$

$$\langle \psi^n \rangle = \int_0^{2\pi} \int_0^\infty \psi^n r dr d\theta.$$

The effective area as defined by Eq. (4) is reasonably close to the fiber core area (A_c). For $V = 2.53$, $A_{\text{eff}} = 1.09A_c$ and for $V = 4.0$, $A_{\text{eff}} = 0.77A_c$. In both cases we assume the modes are the LP_{01} modes of a step-index fiber.

Equation (2) assumes that linear polarization is maintained in the fiber. Actually, the polarization is completely scrambled in both the fibers which reduces δn . We can, however, arrive at a suitable correction factor by averaging the values of δn for linear and circular polarizations. In silica, n_2 is dominated by the electronic contribution so to a good approximation^{8,9}:

$$\delta n(\text{circular}) = \frac{2}{3} \delta n(\text{linear}) \quad (5a)$$

so that

$$\delta n(\text{average}) = \frac{5}{6} \delta n(\text{linear}). \quad (5b)$$

Although we have not done so it is possible to include the effects of a linear chirp on the frequency spectrum. This would be done by multiplying $P(t)^{1/2}$ in Eq. (1) by the term $e^{i\beta t/\tau}$, where β is related to the amount of chirp.¹⁰

Calculated frequency spectra are shown in Fig. 3 for Gaussian pulses with different peak powers. We have plotted the curves for which $\Delta\phi_{\text{max}}$ is in integral units of $\frac{1}{2}\pi$. It can be seen that the photographs in Fig. 2 are in good agreement with the calculated spectra. The photographs in Fig. 2 were taken at powers for which the spectra matched the calculated curves of Fig. 3. The maxima and minima at $\Delta\omega = 0$ do not occur exactly at peak phase shifts of $\frac{1}{2}\pi$, but the error ranges from only 1.5% at 1.5π to 0.3% at 4.5π .

While the measured frequency spectra and those

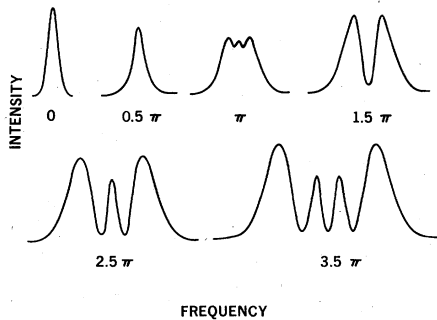


FIG. 3. Calculated frequency spectra for a Gaussian pulse. Spectra are labeled by maximum phase shift at the peak of the pulse.

calculated for a Gaussian pulse agree very well, there is some difference in that the measured spectra show some asymmetry. This asymmetry can be qualitatively understood to arise from asymmetry in the pulse shape. The approximate frequency shift at time (t) is given by the time derivative of the phase perturbation which is proportional to the power.¹

$$\delta\omega(t) = -\frac{\partial\Delta\phi}{\partial t} = -\frac{2\pi L}{\lambda} \frac{\partial\delta n}{\partial t}. \quad (6)$$

Because of SPM the leading edge of the pulse is downshifted in frequency and the trailing edge is upshifted. If the pulse is asymmetric in time the maximum $\delta\omega$ from Eq. (6) will differ between the upshifted and downshifted sides so one would expect an asymmetric broadened spectrum.

One would also expect that non-Gaussian pulses would broaden slightly differently than the spectra for the Gaussian pulse shown in Fig. 3. To examine this question and the effect of asymmetry, we calculated broadened frequency spectra for some non-Gaussian pulses. To do this we choose a pulse which is Gaussian around $x = 0$. The leading or trailing ends, however, can be Gaussian (e^{-x^2}), fall off faster than Gaussian ($ae^{-b|x|^3}$), or fall more slowly than Gaussian ($ce^{-d|x|}$). The constants a , b , c , and d are fixed by requiring continuity of the functions and their derivatives at some particular value of x . In Fig. 4 we plot frequency spectra for several such pulses choosing maximum phase shifts of 1.5π and 4.5π . The functions are given on the left side of the figure. Figures 4(b) and 4(c) show that there are differences between the heights of the sharp inner peaks and

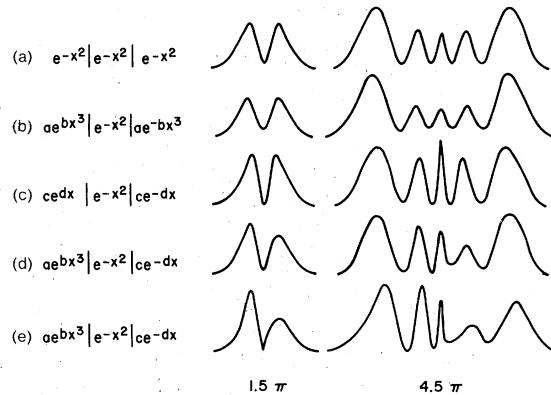


FIG. 4. Comparison of frequency spectra from self-phase-modulation between a Gaussian pulse and a number of non-Gaussian and asymmetric pulses. Only spectra for peak phase shifts of 1.5π and 4.5π are plotted. In (b), (c), and (d) the functions are matched at $x = \pm 1.0$ so $a = e^{-0.333}$, $b = 0.667$, $c = e^{1.0}$, $d = 2.0$. In E the boundary is $x = \pm 0.7$ and $a = e^{-0.1633}$, $b = 0.952$, $c = e^{0.49}$, $d = 1.4$.

the broad outer maxima which depend on whether the tails fall faster or more slowly than the Gaussian pulse. The asymmetric pulse of Fig. 4(d) shows asymmetry mostly in the sharp inner peaks. This is expected because the pulse is symmetric out to $x=1$ so the maximum $\delta\omega$ which occurs for about $|x|=1/\sqrt{2}$ is the same on both the up- and downshifted sides. If, as in Fig. 4(e), we match the functions at $x=\pm 0.707$ there is a difference in the broad peaks as well.

It can be seen from Fig. 4 that the number of peaks depends on the maximum phase shift rather than the shape of the pulse. From Eq. (6) the frequency shift is proportional to the derivative of the instantaneous power and there will generally be two times when the frequency shift is the same. The structure is interpreted as the interference of these different pairs of frequencies.¹ As such, one would expect the number of peaks to depend on peak power and counting the peaks is probably a better measure of the peak power than measuring the frequency width.¹¹

It has been shown that for both Gaussian and Lorentzian pulses there is a simple relation between the pulsewidth, the maximum phase shift, and the width of the broadened spectrum¹² which we rewrite

$$\Delta\tau_p(\text{FW } 1/e) = 1.72\Delta\phi_{\max}/\pi\Delta f, \quad (7)$$

where $\Delta\phi_{\max}$ is obtained from the number of interference peaks as in Fig. 2 and Δf is the $1/e$ full width of the broadened spectrum. If we use Eq. (7) with the spectra for which $\Delta\phi_{\max} > 2.0$, we find $\Delta\tau_p = 155$ ps (FW $1/e$). This number is in excellent agreement with the upper and lower limits discussed in Sec. II.

IV. DETERMINATION OF n_2

The peak power to produce the spectra of Fig. 2 is related to the maximum phase shift by n_2 (which is also the self-focusing coefficient) and various fiber parameters. In Table I we list the average

power coupled into the fiber for the spectra of Fig. 2 which were taken using the $3.35\text{-}\mu\text{m}$ core fiber and for similar spectra taken with the $4.5\text{-}\mu\text{m}$ fiber. The power into the fiber is determined from the output power after correction for fiber loss, reflection loss from the output end, and reflection loss in the output microscope objective. The effective length and effective area for each fiber as calculated from Eqs. (3) and (4) are also included in Table I.

Peak power is derived from average power using the pulse spacing (8.4 ns) and taking a 155-ps (FW $1/e$) Gaussian pulse. Some additional uncertainty arises because of the trailing pulse shown in Fig. 2. At high laser currents this second pulse can be quite strong.¹³ Although we operated at currents where such an additional pulse should not appear, it appears from the photograph that about half the pulse is ringing or reflections in the cables and half is real. At lower laser currents where the trailing pulse should be weaker we see the spectra corresponding to 1.5π and 2.5π at average powers which are about 10% lower than indicated in Table I. We thus reduce the peak power by 10% from the number obtained using the average power, the pulse separation and the pulsewidth so that $P_{\max} = 55.0P_{\text{av}}$.

A value for n_2 was calculated from Eq. (2) for each power reading. We use the correction factor of $\frac{5}{6}$ from Eq. (5b). The refractive index of the fused silica core at 514.5 nm is 1.462. The average value for n_2 from Table I is 1.14×10^{-13} esu with an estimated overall uncertainty of $\pm 15\%$. Note that we assume that n_2 of the 8%- B_2O_3 -92%- SiO_2 cladding does not differ significantly from the value for the pure-silica core.

This value can be compared to other measurements in fused silica. Ellipse rotation gives $n_2 = 1.1 \times 10^{-13}$ esu,^{3,14} measurement of the critical power for self-focusing¹⁵ gives 1.4×10^{-13} and a value of 1.8×10^{-13} is obtained by third-order frequency mixing.¹⁶ It should be noted that these various techniques measure one or more components

TABLE I. Average power coupled into the fiber and resultant value of n_2 for various values of peak phase shift as observed from spectra such as Fig. 2. The average value of n_2 is 1.14×10^{-13} esu. Values for $\Delta\phi_{\max} = \pi$ are neglected in taking the average.

3.35- μm core; $A_{\text{eff}} = 9.61 \times 10^{-8} \text{ cm}^2$ $L = 99 \text{ m}; L_{\text{eff}} = 81.2 \text{ m}$			4.5- μm core; $A_{\text{eff}} = 12.25 \times 10^{-8} \text{ cm}^2$ $L = 116 \text{ m}; L_{\text{eff}} = 77.9 \text{ m}$		
$\Delta\phi_{\max}$	$P_{\text{av}}(i\text{n})$	n_2	$\Delta\phi_{\max}$	$P_{\text{av}}(i\text{n})$	n_2
π	19 mW	1.22×10^{-13} esu	π	21 mW	1.47×10^{-13} esu
1.5π	33	1.05	1.5π	39	1.19
2.5π	50	1.16	2.5π	60	1.28
3.5π	75	1.08	3.5π	102	1.06
4.5π	90	1.16			

of the third-order susceptibility tensor χ_3 . Relating n_2 to these components of χ_3 involves certain approximations which may be valid only to about 15%.¹⁷ Also χ_3 itself contains both electronic and Raman contributions^{3,8} which are weighted slightly differently depending on the specific measurement technique and these corrections are usually ignored. Finally, most of these techniques involve secondary standards such as the Raman cross section of benzene which are themselves uncertain.

An important advantage of the self-phase-modulation measurement of n_2 is that it involves no secondary standards. The present experiment unfortunately does require some assumptions about the components of χ_3 which lead to the correction factor of Eq. (5). This is, however, not a fundamental limitation since we could, in principle, use a birefringent fiber which would maintain polarization¹⁸ so that this correction would not be needed. We could, in fact, use such a birefringent fiber to check the accuracy of Eq. (5b) and thus gain additional information about the components of χ_3 .

V. ANOMALOUS LOW-POWER EFFECTS

When the mode locker is slightly mistuned, we see nonlinear effects on the frequency spectrum at powers well below those where broadening is observed in Fig. 2. Figures 5(a)–5(c) show spectra with slight mistuning of the mode-locker for three powers. The highest power [Fig. 5(c)] corresponds to a maximum phase shift of approximately 0.3π and the power for 5(b) and 5(a) decrease by factors of 2. For comparison, the frequency spectrum of the unbroadened pulse with optimum mode locking is shown in Fig. 5(d). For optimum mode locking there is no change in the frequency spectrum as power is increased until

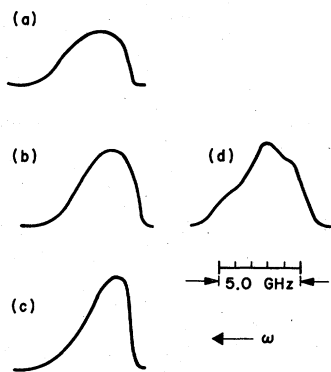


FIG. 5. Intensity-dependent narrowing and asymmetry for slight mode-locker mistuning. Power is increased by a factor of 2 from (a) to (b) and from (b) to (c). (d) shows the spectrum at low powers for optimum mode-locking.

powers corresponding to about 0.5π are reached. This is what would be expected for a Gaussian pulse. Obviously, the measured spectrum is not quite Gaussian. The three-peak structure is probably related to the weak second pulse seen in Fig. 2. The asymmetry in the low-power spectra both in the optimized [5(d)] and mistuned [5(a)] cases is not understood. It is not due to a nonlinear scan of the confocal Fabry-Perot because it is possible to count the individual axial modes of the laser in the spectrum and verify that the scan is indeed linear.

There are two qualitative explanations for the intensity dependent narrowing and asymmetry at these low powers. When the mode locker is slightly mistuned the pulse length is longer than the transform limit and some sort of chirp must exist. One possibility is that SPM in the fiber is canceling some of this chirp and narrowing the frequency spectrum. Another possible explanation is that the low-frequency side of the spectrum is amplified at the expense of the high-frequency side through a low-frequency Raman cross section. A transform-limited pulse could not be narrowed by such a mechanism, but it might be possible to reduce the frequency width of a mistuned pulse.

The difficulty with either of these explanations is that the relevant susceptibilities appear to be too small to explain the observed effects. An intriguing possibility is that we are seeing the effect of a relaxation process in the vicinity of 1 cm^{-1} .

VI. CRITICAL POWER FOR FIBER TRANSMISSION

The combination of frequency broadening from SPM and group velocity dispersion will increase the pulse spreading in a long fiber used for communications. A critical length can be defined where the high frequency part of the pulse is retarded by one pulse length with respect to the low-frequency side. The expression for this critical length is⁶

$$Z_c = [D(\lambda)\delta n_{\max}]^{-1/2} cT_p, \quad (8)$$

where $D(\lambda) = \lambda^2 d^2 n / d\lambda^2$ is the dispersion, cT_p is the pulse length, and δn_{\max} is the maximum index change. If we choose parameters relevant to our $3.35\text{-}\mu\text{m}$ fiber at the maximum phase shift of 4.5π we obtain $z_c = 1.5 \text{ km}$. This justifies our neglect of pulse spreading in the analysis of the data and agrees with the result that the pulse length is unchanged even at the highest powers. In calculating Z_c , δn_{\max} was obtained from $\Delta\phi_{\max} = 4.5\pi$ by using Eq. (2a). The dispersion $D(\lambda) = 0.08$ at 514.5 nm ,¹⁹ and the pulse length is 155 ps . At very high powers self-steepening should occur.²⁰ For the parameters in the present experiment, however, the

self-steepening distance is three orders of magnitude longer than Z_c .⁶

To evaluate the effect of SPM on a single-mode fiber transmission system, it is somewhat simpler to define a critical power rather than a critical length. If the capacity of a single-mode fiber is limited by pulse dispersion, then any additional broadening is undesirable so that we define critical power as that power for which the initial pulse doubles in frequency width. From Fig. 2 the frequency width doubles at $\Delta\phi_{\max} \approx 2.0$ so from Eq. (2)

$$P_c = 10^{-7}(nc\lambda A_{\text{eff}}/4\pi^2 n_2 L) W. \quad (9)$$

Because of linear loss, most of the frequency broadening takes place near the beginning of a long fiber while the pulse spreading takes place along the entire fiber.

The critical power from Eq. (9) for a length of 3.3- μm 17-dB/km fiber would be 180 mW. Note that in this case $L = 1/\alpha = 255$ m from Eq. (3) and we assume the fiber maintains linear polarization. By way of comparison, the critical power for stimulated Raman scattering for the same fiber would be 3 W.⁷ This illustrates that in a high-capacity single-mode fiber SPM may be the dominant nonlinear effect.

VII. CONCLUSION

Frequency broadening from self-phase-modulation has been observed in a single-mode silica core

fiber. The spectrum is in good agreement with that calculated for a simple Gaussian pulse and the nonlinear coefficient agrees well with previous measurements by different techniques.

By defining a critical power as that power for which the initial frequency width doubles it is seen that SPM will be a significant effect at lower powers than the stimulated Raman effect and that SPM will be important in high-capacity single-mode fiber transmission systems.

The results also point to some simple and useful techniques based on fibers for the measurement and analysis of mode-locked laser pulses. Maximizing the frequency width or the number of peaks of the broadened transmitted spectrum provides a simple and sensitive way of "peaking up" the mode-locked drive frequency. The number of interference peaks combined with the frequency width provides an accurate measure of pulse width. Finally, the qualitative features of the broadened spectrum show up asymmetries and deviations from Gaussian behavior of the mode-locked pulse itself.

ACKNOWLEDGMENTS

We are grateful to H. A. Haus for discussions on the theory of self-phase-modulation; to A. Owyong and M. D. Levenson for discussions concerning the self-focusing coefficient; to E. P. Ippen and D. J. Eilenberger for the silicon PIN diode and the pulse-length measurement; and to W. Pleibel for technical assistance.

¹F. Shimizu, Phys. Rev. Lett. **19**, 1097 (1967).

²E. P. Ippen, C. V. Shank, and T. K. Gustafson, Appl. Phys. Lett. **24**, 190 (1974).

³A. Owyong, R. W. Hellwarth and N. George, Phys. Rev. B **5**, 628 (1972).

⁴D. Gloge, Appl. Opt. **10**, 2252 (1971).

⁵T. K. Gustafson, J. P. Taran, H. A. Haus, J. R. Lifszitz, and P. L. Kelley, Phys. Rev. **177**, 306 (1969).

⁶R. A. Fisher and W. K. Bischel, J. Appl. Phys. **46**, 4921 (1975).

⁷R. H. Stolen and E. P. Ippen, Appl. Phys. Lett. **22**, 276 (1973).

⁸A. Owyong, Ph.D. thesis, California Institute of Technology, 1971 (unpublished); Clearinghouse for Federal Scientific and Technical Information Report No. AFOSR-TR-71-3132 (unpublished).

⁹C. C. Wang, Phys. Rev. **152**, 149 (1966).

¹⁰H. A. Haus (private communication).

¹¹P. Cubeddu, R. Polloni, C. A. Sacchi, and O. Svelto, Phys. Rev. A **2**, 1955 (1970).

¹²C. H. Lin and T. K. Gustafson, IEEE J. Quantum Electron. **8**, 429 (1972).

¹³Coherent Radiation instruction manual for Model No. 467 Mode-Locker (unpublished).

¹⁴A. Owyong, IEEE J. Quantum Electron. **9**, 1064 (1973); Opt. Commun. **16**, 266 (1976).

¹⁵W. L. Smith, J. H. Bechtel, and N. Bloembergen, Phys. Rev. B **12**, 706 (1975).

¹⁶M. D. Levenson, IEEE J. Quantum Electron. **10**, 110 (1974).

¹⁷J. J. Song and M. D. Levenson, J. Appl. Phys. **48**, 3496 (1977).

¹⁸E. Snitzer and H. Osterberg, J. Opt. Soc. Am. **51**, 499 (1961); R. H. Stolen and A. Ashkin, Appl. Phys. Lett. **22**, 294 (1973); A. Papp and H. Harms, Appl. Opt. **14**, 2406 (1975).

¹⁹D. Gloge, Appl. Opt. **10**, 2442 (1971).

²⁰F. DiMartini, C. H. Townes, T. K. Gustafson, and P. L. Kelley, Phys. Rev. **164**, 312 (1967).

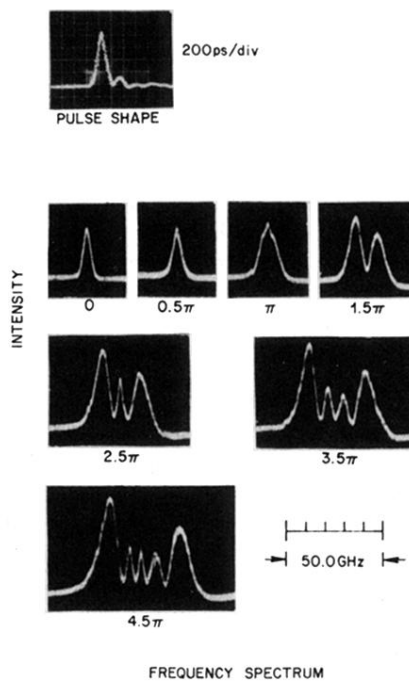


FIG. 2. Photographs of input pulse shape and the output spectrum from a 3.35- μm silica-core fiber. Spectra are labeled by the maximum phase shift which is proportional to peak power.